

## CC chemokine receptor 2 promotes recruitment of myeloid cells associated with insulin resistance in non-alcoholic fatty liver disease

Parker, Richard; Weston, Christopher J; Miao, Zhenhua; Corbett, Christopher; Armstrong, Matthew; Ertl, Linda; Ebsworth, Karen; Walters, Matthew; Baumart, Trageen; Newland, Dale; McMahon, Jeff; Zhang, Penglie; Singh, Rajinder; Campbell, James; Newsome, Philip N; Charo, Israel; Schall, Thomas; Adams, David H

DOI:

[10.1152/ajpgi.00213.2017](https://doi.org/10.1152/ajpgi.00213.2017)

License:

None: All rights reserved

*Document Version*

Peer reviewed version

*Citation for published version (Harvard):*

Parker, R, Weston, CJ, Miao, Z, Corbett, C, Armstrong, M, Ertl, L, Ebsworth, K, Walters, M, Baumart, T, Newland, D, McMahon, J, Zhang, P, Singh, R, Campbell, J, Newsome, PN, Charo, I, Schall, T & Adams, DH 2018, 'CC chemokine receptor 2 promotes recruitment of myeloid cells associated with insulin resistance in non-alcoholic fatty liver disease', *American journal of physiology. Gastrointestinal and liver physiology*, vol. 314, no. 4, pp. G483-G493. <https://doi.org/10.1152/ajpgi.00213.2017>

[Link to publication on Research at Birmingham portal](#)

**Publisher Rights Statement:**

Checked for eligibility: 15/03/2018  
<https://doi.org/10.1152/ajpgi.00213.2017>

**General rights**

Unless a licence is specified above, all rights (including copyright and moral rights) in this document are retained by the authors and/or the copyright holders. The express permission of the copyright holder must be obtained for any use of this material other than for purposes permitted by law.

- Users may freely distribute the URL that is used to identify this publication.
- Users may download and/or print one copy of the publication from the University of Birmingham research portal for the purpose of private study or non-commercial research.
- User may use extracts from the document in line with the concept of 'fair dealing' under the Copyright, Designs and Patents Act 1988 (?)
- Users may not further distribute the material nor use it for the purposes of commercial gain.

Where a licence is displayed above, please note the terms and conditions of the licence govern your use of this document.

When citing, please reference the published version.

**Take down policy**

While the University of Birmingham exercises care and attention in making items available there are rare occasions when an item has been uploaded in error or has been deemed to be commercially or otherwise sensitive.

If you believe that this is the case for this document, please contact [UBIRA@lists.bham.ac.uk](mailto:UBIRA@lists.bham.ac.uk) providing details and we will remove access to the work immediately and investigate.

Download date: 19. Apr. 2024

1 CC Chemokine Receptor 2 Promotes  
2 Recruitment of Myeloid Cells Associated with  
3 Insulin Resistance in Non-Alcoholic Fatty Liver  
4 Disease

5 Richard Parker<sup>1</sup>, Christopher Weston<sup>1</sup>, Zhenhua Miao<sup>2</sup>, Christopher Corbett<sup>3</sup>, Matthew  
6 Armstrong<sup>1</sup>, Linda Ertl<sup>2</sup>, Karen Ebsworth<sup>2</sup>, Matthew Walters<sup>2</sup>, Trageen Baumart<sup>2</sup>, Dale  
7 Newland<sup>2</sup>, Jeff McMahon<sup>2</sup>, Penglie Zhang<sup>2</sup>, Rajinder Singh<sup>2</sup>, James Campbell<sup>2</sup>, Philip  
8 Newsome<sup>1</sup>, Israel Charo<sup>2</sup>, Thomas Schall<sup>2</sup>, David H Adams<sup>1</sup>

9

- 10 1. NIHR Biomedical Research Unit and Centre for Liver Research, University of  
11 Birmingham, Birmingham, United Kingdom  
12 2. ChemoCentryx Inc, Mountain View, California USA  
13 3. Royal Wolverhampton Hospitals NHS Foundation Trust, Wolverhampton UK

14

15

16 Running head: CCR2 in NAFLD

17

18 Corresponding author:

19 Dr Richard Parker

20 richardparker@nhs.net

21 NIHR Centre for Liver Research

22 5<sup>th</sup> Floor IBR

23 University of Birmingham

24 Birmingham

25 B15 2TT

26 United Kingdom

27 Telephone (44) (0) 7971118036

28 Fax (44) (0) 121 415 8701

29

30 List of abbreviations

ALT	Alanine aminotransferase
ANOVA	Analysis of variance
AST	Aspartate aminotransferase
CCL2	CC chemokine ligand 2
CCR2	CC chemokine receptor 2
ELISA	Enzyme linked immunosorbent assay
FACS	Flow assisted cytometry
HFD	High fat diet
NAFLD	Non-alcoholic Fatty Liver Disease
NAS	NAFLD activity score
NASH	Non-alcoholic steatohepatitis
PBS	Phosphate buffered saline
RNA	Ribonucleic acid
rt-PCR	Real time polymerase chain reaction
SEM	Standard error of mean

31

32

33 Financial Support: RP received support from a Clinical Research Training Fellowship from  
34 the Medical Research Council grant number G1100448, and a Sheila Sherlock Travelling  
35 Fellowship in Hepatology awarded by the Royal College of Physicians, London.  
36 ChemoCentryx Inc designed and developed the small molecule inhibitor of chemokine-C-  
37 receptor 2, CCX872, which is a proprietary compound.

38

39

40 Author contributions:

41 RP designed and performed experiments and analysis, wrote the draft manuscript

42 CW designed experiments, analysed data and reviewed the draft manuscript

43 CC collected human samples, performed experiments and reviewed the draft manuscript

44 MA collected samples and reviewed the draft manuscript

45 LE, KE, TB assisted with animal experiments

46 ZM, DN, JM, PZ, RS medicinal chemistry

47 MW, JC, PN, IC, TS and DA designed experiments, analysed data and reviewed the draft  
48 manuscript.

49 All authors reviewed the final manuscript and approved its submission

50

51 Conflicts of interest

52 RP: no conflict of interest  
53 CW: no conflict of interest  
54 CC: no conflict of interest  
55 MA: no conflict of interest  
56 LE: employee of ChemoCentryx Inc.  
57 KE: employee of ChemoCentryx Inc.  
58 TB: employee of ChemoCentryx Inc.  
59 ZM: employee of ChemoCentryx Inc.  
60 DN: employee of ChemoCentryx Inc.  
61 JM: employee of ChemoCentryx Inc.  
62 PZ: employee of ChemoCentryx Inc.  
63 RS: employee of ChemoCentryx Inc.  
64 MW: no conflicts of interest  
65 JC: employee of ChemoCentryx Inc.  
66 PN: no conflicts of interest  
67 IC: employee of ChemoCentryx Inc.  
68 TS: employee of ChemoCentryx Inc.  
69 DA: no conflicts of interest

70 **Abstract**

71 Non-alcoholic fatty liver disease (NAFLD) is a common disease, closely associated with obesity and  
72 insulin resistance. We investigated the presence of a subset of myeloid cells associated with metabolic  
73 disturbance in the liver of patients with NAFLD and a murine model of obesity-induced liver disease.  
74 Gene and protein expression in liver and serum was investigated with rt-PCR or ELISA and correlated  
75 to clinical disease. Liver-infiltrating immune cells were isolated from normal or diseased human liver  
76 for flow cytometric analysis. In animal experiments, mice were fed a high-fat diet (60% of calories  
77 from fat) for 16 weeks, or high-fat diet with 30% fructose for 32 weeks to induce steatohepatitis and  
78 fibrosis. A small molecule inhibitor of CCR2, CCX872, was administered to some mice. A subset of  
79 CD11c<sup>+</sup>CD206<sup>+</sup> immune cells were enriched in human liver tissue, and greater infiltration was  
80 observed in NAFLD. The presence of CD11c<sup>+</sup>CD206<sup>+</sup> myeloid cells correlated with systemic insulin  
81 resistance. CD11c<sup>+</sup>CD206<sup>+</sup> cells expressed high levels of CCR2, and liver CCL2 expression was  
82 increased in NASH and correlated with disease activity. In mice, CCR2 inhibition reduced infiltration  
83 of liver CD11b<sup>+</sup>CD11c<sup>+</sup>F4/80<sup>+</sup> monocytes, which are functional homologs of human CD11c<sup>+</sup>CD206<sup>+</sup>  
84 cells, and improved liver injury and glycaemic control. A role for CCR2/CCL2 in human NAFLD has  
85 long been postulated. These data confirm a role for this chemokine/receptor axis, through mediating  
86 adipose and hepatic infiltration of myeloid cells. Inhibition of CCR2 improved hepatic inflammation  
87 and fibrosis in murine models of NAFLD. These data confirm the rationale for targeting CCR2 to  
88 treat NAFLD.

89

90 **New and noteworthy**

91 These data show for the first time that CD11c<sup>+</sup>CD206<sup>+</sup> myeloid cells, previously associated with  
92 human adipose tissue inflammation, infiltrate into liver tissue in non-alcoholic fatty liver disease. These  
93 cells express CCR2. Inhibition of CCR2 in mice inhibits hepatic inflammation caused by a murine  
94 homolog of these myeloid cells and improves experimental liver disease.

95

96 **Keywords:**

- 97 1. Non-alcoholic fatty liver disease
- 98 2. Immunology
- 99 3. Obesity
- 100 4. Insulin resistance
- 101 5. Immunology

102

## 103 CC Chemokine Receptor 2 Promotes 104 Recruitment of Myeloid Cells Associated with 105 Insulin Resistance in Non-Alcoholic Fatty Liver 106 Disease

107 Non-alcoholic fatty liver disease (NAFLD) covers a spectrum of liver pathology from hepatic  
108 steatosis (non-alcoholic fatty liver, NAFL) through the more severe non-alcoholic  
109 steatohepatitis (NASH) to cirrhosis (31). NAFLD is present in up to one-third of individuals  
110 (6) and is associated with the metabolic syndrome, particularly obesity (31) and insulin  
111 resistance (3). NAFLD is becoming the commonest indication for liver transplantation in the  
112 USA (32) reflecting both the prevalence of the disease and the present lack of  
113 effective therapies for advanced disease (25).

114 There is increasing interest in the role of the innate immune system in obesity and the  
115 metabolic syndrome. Myeloid cells infiltrate adipose and liver tissue in patients with NAFLD  
116 and secrete cytokines and adipokines that contribute to insulin resistance and inflammation.  
117 In particular, CD11c<sup>+</sup>CD206<sup>+</sup> monocytes in human adipose tissue are associated with  
118 adipocyte necrosis, inflammation and insulin resistance (30). In mice, a functionally similar  
119 subset defined by CD11b<sup>+</sup>CD11c<sup>+</sup>F4/80<sup>+</sup> contribute to adipose inflammation and systemic  
120 insulin resistance in mice (22, 26). CCR2 mediates obesity-associated macrophage  
121 infiltration of adipose and hepatic tissue (19, 29). Mouse experiments have demonstrated  
122 that obesity increases hepatic expression of CCL2 (13, 14, 23, 29) and  
123 CD11b<sup>+</sup>CD11c<sup>+</sup>F4/80<sup>+</sup> express CCR2 (26). Inhibition of the CCR2/CCL2 axis reduces  
124 disease activity in mice (21, 27, 33)(4, 8). The CCR2/CCL2 axis in human NAFLD is less  
125 well defined, although increased circulating levels of CCL2 are observed (12, 14). We  
126 investigated the inflammatory infiltrate in human NAFLD and murine models of obesity-

127 induced liver disease to determine whether functionally important subsets of CCR2  
128 inflammatory cells are involved in the metabolic dysfunction that characterises NAFLD.

## 129 **Materials and methods**

### 130 Human tissue

131 Human tissue and blood was collected from patients with liver disease or healthy controls at  
132 University Hospitals Birmingham NHS Foundation Trust with full informed consent and  
133 research ethics committee approval (REC reference 06/Q2708/11). Liver tissue was  
134 obtained from patients undergoing hepatic resection for benign or malignant disease, or liver  
135 transplantation for chronic liver disease. In the case of hepatic resection, liver tissue distal to  
136 resected lesions was used for analysis. No patient had undergone chemotherapy in the two  
137 weeks prior to surgery. Liver tissue was placed in formalin or snap frozen prior to  
138 subsequent analysis. Characteristics of these groups and of patients undergoing resection or  
139 transplantation as a source of liver tissue are detailed in **table 1**. Serum from patients with  
140 NAFLD was obtained from 2 cohorts of patients taking part in the LEAN and NOBLES  
141 studies. LEAN is a randomised controlled trial of liraglutide in patients with NAFLD (2). The  
142 serum samples used were taken before randomisation. NOBLES is an observational study of  
143 biomarkers in patients with liver disease. Finally, a group of healthy volunteers without liver  
144 disease donated blood for analysis and served as a control group in ELISA experiments. This  
145 group were drawn from laboratory colleagues and gave consent for their samples to be used  
146 for research.

### 147 Enzyme Linked Immunosorbent Assays (ELISA)

148 Analysis of human serum was performed using commercially available ELISA kits. Serum  
149 CCL2 concentration was measured using R&D Systems Quantikine kits (Minneapolis,  
150 Minnesota USA, catalogue number PDCP00), performed according to the manufacturer's  
151 instructions. Recombinant human chemokines were used as a positive control (Peprotech,



152 New Jersey USA). Samples were diluted in sample buffer 1:4 and run in duplicate. A standard  
153 curve was generated from known concentrations of recombinant chemokine and  
154 experimental values interpolated from this curve.

155

#### 156 Polymerase Chain Reaction

157 RNA was isolated by homogenizing liver tissue in Trizol (Life Technologies, California, USA).

158 Chloroform was added and samples centrifuged at top speed in a microfuge for 15 minutes.

159 The upper aqueous layer was removed, isopropanol was added and samples centrifuged at

160 12,000rpm for 15 minutes. The resulting RNA pellet was washed in 70% ethanol and re-

161 suspended in nuclease free water. Purity and concentration of total RNA was determined

162 spectrophotometrically. cDNA was prepared from RNA using Taqman reagents (Life

163 Technologies, California, USA) according to the manufacturer's instructions. Briefly, 2  $\mu$ L of

164 RNA was combined with random hexamers, reverse transcriptase, RNase inhibitor,

165 magnesium chloride and a buffer solution. This mixture was heated to 25°C for 10 minutes,

166 37°C for 30 minutes, 95°C for 5 minutes and then cooled to 4°C. Probe/primer mixes for

167 genes of interest and appropriate controls were obtained from Taqman (Life Technologies,

168 California, USA) and made up with Taqman reagents. A 96 well plate was used for reactions,

169 with wells containing cDNA, primer/probe mix (*CCL2* primer/probe mix catalogue number

170 Hs00234140\_m1, *18S* mix catalogue number Hs03003631\_g1) and Taqman mastermix.

171 Three replicates were used for both the gene of interest and housekeeping gene. *18S* has

172 been shown to have lowest level of variability across stages of alcoholic liver disease (ALD)

173 suggesting it is reliable as a housekeeping gene in steatohepatitis (5). PCR experiments were

174 performed using a Roche Lightcycler 480 machine. A single quantification measurement was

175 taken during each cycle.

176 Isolation of leukocytes

177 *Isolation of leukocytes from human liver or blood*

178 Mononuclear cells were isolated from blood or liver. Liver was washed with phosphate  
179 buffered saline (PBS) to remove blood and digested non-enzymatically using GentleMACS  
180 (Miltenyi). The resulting homogenate was passed through a sterile 70 micron mesh . The  
181 homogenate was then washed in PBS until a clear supernatant was achieved. Liver  
182 homogenate or whole blood was layered over a density gradient (Lymphoprep, CedarLane  
183 Labs, Canada) to isolate mononuclear cells, which were aspirated from the interface and  
184 washed in PBS three times before further analysis.

185 *Isolation of leukocytes from murine liver tissue*

186 Mice were sacrificed by CO<sub>2</sub> inhalation and cervical dislocation. Blood samples were taken  
187 by left ventricular puncture. PBS was gently infused into the left ventricle to flush end organs  
188 of blood before harvesting. The liver were removed, immediately divided and placed into  
189 RPMI, formalin or snap frozen in liquid nitrogen. To isolate leukocytes, a segment of liver  
190 was coarsely chopped with scissors before mechanical dissociated by gently passing  
191 homogenate through a 75-micron sieve. The resulting homogenate was washed in PBS until a  
192 clear supernatant was achieved. For analysis of mouse liver, whole homogenate was  
193 incubated with fluorescently-tagged antibodies as described below, and CD45 used to  
194 identify leukocytes.

195 Flow Cytometry analysis of leukocytes

196 Isolated cells were suspended in 100µL at 1x10<sup>6</sup> cells/ml in MACS buffer (PBS containing 2%  
197 FCS and 1mM EDTA) and incubated with antibodies. After incubation for 20 minutes at  
198 room temperature, cells were washed and re-suspended in PBS and analysed by flow  
199 cytometry using a Beckman Coulter Cyan. Cells stained with single colours were analysed  
200 for compensation and appropriate isotype controls were used to define the negative  
201 populations.

202 Animal experiments

203 Mouse experiments were performed at ChemoCentryx Inc, California, USA. C57/Bl6 mice  
204 were purchased from Charles River, USA, and were housed in the research locations for at  
205 least three days before investigations were started. Animals were housed according to local  
206 and national standards. Animal housing was maintained at 23°C with twelve hour light/dark  
207 cycles. Male C57/Black 6 (C57/Bl6) mice bred in controlled clean conditions were used for  
208 all experiments, aged 6-8 week at the start of experiments.

209 Two animal models were used: high fat diet (HFD) to induce steatohepatitis, or HFD in  
210 combination with 30% fructose in drinking water to induce steatohepatitis with fibrosis. The  
211 HFD provided 60% of calories from fat (by overall weight, this is provided 31% by lard and  
212 3% by soybean oil). HFD and control diet were obtained from Teklad, USA. HFD was  
213 administered for 16 weeks; HFD+fructose was administered for 32 weeks. In each case, a  
214 control group of littermates were fed control diet (10% of calories from fat) with normal  
215 drinking water for the duration of the experiment. At the end of experiments mice were  
216 sacrificed by CO<sub>2</sub> inhalation.

217 *Chemokine receptor antagonism*

218 A small molecule inhibitor of CCR2 (CCX872) manufactured by ChemoCentryx Inc,  
219 Mountain View, USA. CCX872 was dissolved in 1% hydroxypropyl methylcellulose (HPMC)  
220 and administered to mice by subcutaneous injection at a dose of 30mg/kg daily. An  
221 equivalent volume of 1% HPMC was given in control experiments. A maximum volume of  
222 350µL was used.

223 *Triglyceride content of murine liver tissue*

224 Triglyceride content of murine liver tissue was assessed using a commercially available  
225 colorimetric assay kit (Cayman Chemical Company, Ann Arbor MI USA) according to the  
226 manufacturer's instructions. In short, 400mg of liver tissue was suspended in 2ml of assay  
227 diluent and homogenised. 10µl of homogenate was added to wells of a 96 well plate, each  
228 sample was assayed in triplicate. Triglycerides were enzymatically hydrolysed to free fatty

229 acids and glycerol using the supplied enzyme mixture. After 15 minutes incubation colour  
230 change was measured with a plate reader (Synergy HT, BioTek, Vermont, USA) by  
231 measuring absorbance at 540nm. A standard curve was generated by assaying known  
232 concentrations of triglyceride and the triglyceride concentration of samples interpolated  
233 from this curve and expressed as milligram per gram of liver tissue.

#### 234 *Fibrosis content of liver tissue*

235 Entire lobes of mouse livers were immersed in formalin immediately after harvesting and  
236 subsequently embedded in paraffin. Sections of 10 µm thickness were stained with Sirius red  
237 (Sigma Aldrich, Missouri, USA) to detect collagen deposition. Briefly, sections were dewaxed  
238 and stained with haematoxylin before being stained with Sirius red for 1 hour. Sections were  
239 then dehydrated and mounted. Fibrosis was quantified by calculating percentage area of  
240 collagen deposition using Image-J software (National Institutes of Health, USA; version 1.48).  
241 Two Sirius red-stained slides per animal were taken at different depth, with 18 images taken  
242 randomly per slide for a total of 36 images per animal for collagen quantification. All  
243 pathologic evaluations were made by a pathologist on a random and blinded basis.

#### 244 Glycaemic control

245 Glucose metabolism in mice was assessed with insulin and glucose challenge experiments.  
246 Insulin challenge was performed by administering 0.75U/kg of insulin (Sigma Aldrich, USA) to  
247 non-fasted mice via intra-peritoneal injection. Plasma glucose was measured with an  
248 AccuCheck glucometer (Roche, Basel, Switzerland) using a drop of blood from a tail vein.  
249 Plasma glucose was measured at baseline and 15, 30, 60, 90 and 120 minutes following  
250 administration of insulin. Mice were fasted overnight before glucose tolerance tests. Glucose  
251 (Sigma Aldrich, USA) was administered at 2g/kg of glucose (as 45% glucose solution), given  
252 by gastric lavage. Plasma glucose was measured at baseline and 15, 30, 60, 90 and 120  
253 minutes after administration of glucose using an AccuCheck glucometer and drops of blood  
254 from tail vein.

255 Statistical Analysis

256 Data are expressed as mean and SEM for normally expressed data, and median and  
257 interquartile range (IQR) for skewed data. Normality was assessed with the Kolmogorov-  
258 Smirnov test. Normally distributed data were compared between groups with student's t-  
259 test, and the Mann-Whitney test used for skewed data. Variance across multiple groups, for  
260 example over a range of concentrations was analysed with one-way analysis of variance  
261 (ANOVA). Survival analysis was analysed by Kaplan-Meier curves with p values assessed with  
262 log-rank test. Median time to death in animals that died was also calculated. All authors had  
263 access to the study data and reviewed and approved the final manuscript. Data were  
264 analysed using Prism version 5 (California, USA).

265 **Results**

266 CD14<sup>+</sup>CD11c<sup>+</sup>CD206<sup>+</sup> monocytes are enriched in NAFLD liver tissue

267 Immune cells that express CD14<sup>+</sup>CD11c<sup>+</sup>CD206<sup>+</sup> have been detected in human adipose  
268 tissue and associated with insulin resistance (30). We examined the presence of these cells  
269 in human blood and liver. Liver tissue from patients with NAFLD (n=8), other liver disease  
270 (ALD n=4, PSC n=3, PBC n=2, cryptogenic cirrhosis n=1, haemochromatosis n=1) or  
271 without liver disease (n=5) was analysed. Very few CD14<sup>+</sup>CD11c<sup>+</sup>CD206<sup>+</sup> were observed in  
272 peripheral blood, whereas these cells were enriched in liver tissue (**figure 1**). The frequency  
273 of intrahepatic CD11c<sup>+</sup>CD206<sup>+</sup> monocytes, as a percentage of CD45<sup>+</sup>CD14<sup>+</sup> cells, differed  
274 significantly between types of liver disease (Kruskal-Wallis p=0.023) with highest frequency  
275 of cells seen in NAFLD (**figure 1E**). Mean fluorescence intensity (MFI) of CD11c and  
276 CD206 showed a tendency to be greater in NAFLD, although this did not reach statistical  
277 significant (Kruskal-Wallis p=0.056) (**figure 1F**). No differences in expression of CD11c and  
278 CD206 were seen between non-cirrhotic and cirrhotic liver tissue (data not shown).

279 CD14<sup>+</sup>CD11c<sup>+</sup>CD206<sup>+</sup> monocytes are associated with insulin resistance and express CCR2  
280 in NAFLD

281 A correlation between the proportion of intrahepatic CD14<sup>+</sup>CD11c<sup>+</sup>CD206<sup>+</sup> monocytes  
282 and glycosylated haemoglobin (HbA1c) was observed in liver infiltrating monocytes isolated  
283 from patients with chronic liver disease ( $r^2$  0.499  $p=0.0005$ ) (**figure 2A**). No significant  
284 correlation was observed with age, BMI or ALT (**table 2**). In both blood and liver, CCR2  
285 expression was largely restricted to CD14<sup>+</sup> monocytes particularly the classical  
286 CD14<sup>++</sup>CD16<sup>-</sup> subset (**figure 2B**). The overall frequency of CCR2<sup>+</sup> cells in blood or liver  
287 tissue did not vary significantly by aetiology of liver disease (one-way ANOVA  $p=0.236$ ).  
288 However, CCR2<sup>+</sup> expression on CD14<sup>+</sup>CD11c<sup>+</sup>CD206<sup>+</sup> monocytes was higher in NAFLD  
289 compared to normal liver tissue or non-NAFLD liver disease in terms of the percentage of  
290 CD14<sup>+</sup>CD11c<sup>+</sup>CD206<sup>+</sup> cells that expressed CCR2 (**figure 3A**) and the MFI of CCR2  
291 (**figure 3B**).

292 CCL2 is upregulated in NAFLD

293 *CCL2* gene expression in liver tissue was analysed by quantitative real-time PCR using *18S* as  
294 a housekeeping gene. *CCL2* gene expression was significantly up regulated in liver tissue from  
295 patients with NAFLD undergoing transplantation (Mann Whitney test  $p=0.009$ ) (**figure 4A**).  
296 The concentration of CCL2 was measured by ELISA in serum of individuals with biopsy-  
297 proven NAFLD ( $n=20$ ) or healthy volunteers ( $n=10$ ). Serum CCL2 concentration was  
298 significantly higher in patients with NAFLD compared to healthy volunteers (median  
299 305.1pg/ml (IQR 211.8 – 385.7) vs. 224.7 (105.2 – 255.4), Mann-Whitney test  $p=0.021$ )  
300 (**figure 4B**). NAFLD was assessed histologically by independent pathologists using the  
301 NAFLD activity score (NAS) proposed by Kleiner and Brunt (15). Serum CCL2  
302 concentration was higher in individuals with more severe histological inflammation (assessed  
303 with the NAFLD activity score (NAS) (15))(one way ANOVA  $p=0.025$ ) but levels did not  
304 correlate with fibrosis stage (one way ANOVA  $p=0.347$ ) (**figure 4C, D**). When  
305 individual components of the NAS were considered, serum CCL2 concentration was

306 associated with higher lobular inflammation score (one-way ANOVA  $p=0.043$ ) but not with  
307 steatosis or hepatocyte ballooning, consistent with the known role of CCL2 as a monocyte  
308 chemo-attractant.

309 Inhibition of CCR2 reduces accumulation of F4/80<sup>+</sup>CD11c<sup>+</sup> monocytes in murine  
310 steatohepatitis

311 CD11b<sup>+</sup> CD11c<sup>+</sup>F4/80<sup>+</sup> monocytes are found in adipose tissue in experimentally induced  
312 obesity in mice, and are functionally similar to CD11c<sup>+</sup>CD206<sup>+</sup> monocytes in humans. To  
313 investigate the effect of CCR2 inhibition in obesity-induced steatohepatitis, twenty-six male  
314 C57/Bl6 mice were given HFD with 60% of calories from fat for 16 weeks. After eight weeks  
315 of HFD, the mice were divided into two groups: thirteen were treated daily with CCX872  
316 (30mg/kg/day, administered by subcutaneous injection) and 13 received an equivalent volume  
317 of vehicle (1% HPMC). A further 8 littermates were given control diet for the duration of  
318 the experiment.

319 Steatosis, assessed by measuring triglyceride content of liver tissue, was markedly increased  
320 after 16 weeks of HFD. Mice treated with CCX872 had significantly less triglyceride  
321 accumulation in comparison with vehicle treated mice (169.6mg/g  $\pm$ 21.20 vs. 284.2  $\pm$ 31.9,  
322 student's t-test  $p=0.007$ ) with levels reduced to those seen in animals receiving a control  
323 diet (**figure 5A**). Serum ALT was significantly lower in CCX872-treated mice (mean ALT  
324 252.5IU/ml  $\pm$ 56.02 vs. 532.8  $\pm$ 98.07, student's t-test  $p=0.028$ ) (**figure 5B**). The reduction in  
325 hepatic steatosis was confirmed histologically (**figure 5C**) but histological features of  
326 inflammation and fibrosis did not differ between groups (**figure 5D, E**).

327 Flow cytometric analysis of isolated liver-infiltrating immune cells revealed an increase in  
328 CD11b<sup>+</sup>F4/80<sup>low</sup> cells in all HFD fed mice. No differences were seen between groups with  
329 regard to intrahepatic frequencies of CD11b<sup>+</sup>F4/80<sup>hi</sup> Kupffer cells or overall CD11b<sup>+</sup>F4/80<sup>low</sup>  
330 infiltrating monocytes (**figure 6A, B**). However, fewer CCR2 expressing monocytes were  
331 seen in CCX872 treated mice (**figure 7A**) and CCR2 inhibition reduced liver infiltration  
332 with Ly6<sup>chi</sup> monocytes (**figure 7B**). HFD feeding resulted in higher intrahepatic and adipose

333 tissue frequencies of CD11b<sup>+</sup> CD11c<sup>+</sup>F4/80<sup>+</sup> cells, an immune cell population functionally  
334 similar to CD11c<sup>+</sup>CD206<sup>+</sup> cells in humans which are implicated in the development of  
335 obesity mediated insulin resistance (19). The frequency of CD11b<sup>+</sup>CD11c<sup>+</sup>F4/80<sup>+</sup> cells in  
336 both adipose and liver tissue was significantly reduced after treatment with CCX872 (**figure**  
337 **6C, D**).

#### 338 Inhibition of CCR2 reduces scarring in murine steatohepatitis and fibrosis

339 Only mild hepatic fibrosis was seen after 16 weeks of HFD (figure 7E). As fibrosis is an  
340 important prognostic marker in human NAFLD (1, 9) we sought to assess the effects of  
341 CCR2 antagonism on the development of fibrosis. Fructose intake is associated with more  
342 severe fibrosis in human NAFLD (24) and has been shown to cause fibrosis in animal models  
343 of NAFLD (7, 16). We used HFD and fructose to induce fibrosis and assess the effect of  
344 CCR2 antagonism. Twenty-two mice were given HFD and 30% fructose for 32 weeks.  
345 CCX872 or vehicle was administered daily for the final eight weeks of the experiment, each  
346 to 11 mice. A further four littermates were given control diet for the duration of the  
347 experiment.

348 Consistent with initial experiments, after 32 weeks lower ALT concentrations were  
349 observed in CCX872-treated animals (median 67.0 IU/L vs. 251.5IU/L,  $p < 0.006$  by Mann  
350 Whitney test) although interestingly, lower than seen after a shorter period of HFD diet  
351 alone. Hepatic fibrosis, assessed by area of scarring on histology, was significantly reduced in  
352 the livers of mice receiving CCX872 (mean area 0.83 % (SD 0.22) vs. 2.01 (1.5),  $p = 0.01$  by  
353 student's t-test) (**figure 8**).

#### 354 CCR2 antagonism improves glucose metabolism in mice given HFD

355 At the start of the treatment period (after eight weeks of HFD), response to a glucose load  
356 was similar between CCX872 and vehicle treated mice (**figure 9A, C**). However, after 8  
357 weeks of treatment there was a significant improvement in response of CCX872 mice  
358 compared to vehicle treated mice (AUC 48545 mg/dl/min vs. 31795 mg/dl/min, student's t-



359 test  $p < 0.001$ ) (**figure 9B, C**). Insulin challenge was performed by administering a standard  
360 dose of 0.75units/g of insulin by intra-peritoneal injection to non-fasted mice. At the start of  
361 the treatment period changes in plasma glucose concentration in response to insulin were  
362 similar in both groups of mice fed HFD (**figure 9D, F**). After a further 8 weeks of HFD and  
363 treatment with CCX872 or vehicle, there was a significant difference between groups (AUC  
364 21719 mg/dl/min vs. 16553 mg/dl/min, student's t-test  $p < 0.001$ ) (**figure 9D,F**).

## 365 **Discussion**

366 Non-alcoholic fatty liver disease is a common condition closely related to obesity and the  
367 metabolic syndrome. Progressive disease is typified by hepatic inflammation in the form of  
368 steatohepatitis and fibrosis (11). We report here that a subset of monocytes that express  
369 both CD11c and CD206 are enriched in the liver of patients with NAFLD and their  
370 presence is associated with insulin resistance. A similar subset has been reported previously  
371 in human adipose tissue but not in liver tissue (30). We show that intrahepatic  
372 CD11c<sup>+</sup>CD206<sup>+</sup> monocytes express CCR2, and its principal ligand, CCL2, is over-expressed  
373 in NAFLD liver tissue suggesting that the CCR2/CCL2 axis may promote trafficking of  
374 CD11c<sup>+</sup>CD206<sup>+</sup> monocytes to the liver in NAFLD which would suggest targeting CCR2  
375 therapeutically may be of benefit in NAFLD.

376

377 To test this hypothesis we investigated the role of CCR2 in trafficking of pro-inflammatory  
378 myeloid cells in a mouse model of non-alcoholic fatty liver disease where high fat diet feeding  
379 causes insulin resistance, steatohepatitis and hepatic fibrosis. When a small molecule  
380 inhibitor of CCR2 was administered to mice the numbers of liver and adipose tissue  
381 infiltrating CD11b<sup>+</sup>CD11c<sup>+</sup>F4/80<sup>+</sup> cells was reduced, accompanied by improvements in liver  
382 histology and glycaemic control.

383

384 The transition from simple steatosis to NASH is associated with hepatic inflammation and  
385 the development of insulin resistance even in the absence of overt diabetes mellitus. The  
386 present study suggests that a specific subset of liver tissue infiltrating monocytes provide the  
387 link between hepatic inflammation and insulin resistance. Wentworth et al. reported that the  
388 presence of pro-inflammatory CD11c<sup>+</sup>CD206<sup>+</sup> monocytes in subcutaneous and omental  
389 adipose tissue of obese individuals (30) was associated with insulin resistance. This was  
390 mediated in part through the inhibition of the action of insulin on adipocytes. We now  
391 report the same subset of monocytes in the livers of patients with NASH. In contrast to  
392 Wentworth we detected high levels of CCR2 on CD11c<sup>+</sup>CD206<sup>+</sup> cells in the liver. A  
393 comparable subset of monocytes in mice is defined by F4/80 and CD11c expression. These  
394 cells express CCR2 and use it to infiltrate adipose tissue (19). Our data confirm and extend  
395 these observations by showing that pharmacological inhibition of CCR2 reduces not only  
396 adipose tissue infiltration but also hepatic infiltration by this subset. A crucial role for these  
397 cells in disease pathogenesis was suggested by our finding of a strong correlation between  
398 the frequency of CD11c<sup>+</sup>CD206<sup>+</sup> cells in the liver and clinical measurement of insulin  
399 resistance. Thus local hepatic insulin resistance may be mediated in part through  
400 inflammation caused by this monocyte subset recruited to the liver in response to increased  
401 CCL2 expression. Thus, the improvement in glucose metabolism observed in mice is likely to be  
402 multi-factorial. Improved adipose tissue inflammation will improve insulin resistance at this site,  
403 while reduced hepatic inflammation is also likely to improve hepatic glucose metabolism.

404

405 There have been several studies that examine the CCR2/CCL2 axis in the murine models of  
406 liver disease. Inhibition of CCR2/CCL2 either through genetic manipulation (23, 29) or  
407 pharmaceutical targeting (4, 17, 21, 27, 33) leads to improvements in steatosis,  
408 inflammation or fibrosis with variation dependent on the model employed. Many of  
409 these pre-clinical pharmaceutical studies have relied on transgenic mice (28, 33) used

410 non-physiological methods such as administration of carbon tetrachloride (4) or  
411 streptozotocin (17), or deficient diets (4, 21) and as such are of limited translational value.  
412 Our data presented here deliberately used diets that mimic high-fat and /or high-  
413 carbohydrate diets which are a feature of human liver disease. This is a particular contrast to  
414 the study by Lefebvre et al (17) who induced NASH in part by using streptozotocin to kill  
415 pancreatic islet cells.

416

417 Increased CCL2 expression in human NAFLD has been described previously by Haukeland  
418 et al. (12) who reported higher levels of circulating CCL2 in NAFLD and in progressive  
419 disease. Our data confirm this finding and by correlating CCL2 blood levels with histological  
420 features seen on liver biopsies taken at the same time show that CCL2 expression  
421 correlates with hepatic inflammation but not fibrosis. We also show increased liver-specific  
422 expression of CCL2 in patients with NAFLD although this data has limitations through the  
423 number of samples used for analysis of liver-specific CCL2 expression, and the necessary  
424 reliance of samples from patients with advanced disease to analyse liver inflammation. CCL2  
425 is the major chemokine ligand for the receptor CCR2 which mediates myeloid cell trafficking  
426 into tissues. Intrahepatic monocytes as a group express low levels of CCR2 but this is not  
427 the case for CD11c<sup>+</sup>CD206<sup>+</sup> monocytes which maintain high levels of CCR2 suggesting that  
428 CCL2/CCR2 interactions may be more important for the recruitment and positioning of  
429 these cells in liver tissue. Based on these findings we hypothesised that inhibiting CCR2  
430 would reduce transmigration of monocytes into adipose and liver tissue. This was confirmed  
431 in mice where inhibition of CCR2 using a small molecule CCR2 inhibitor reduced  
432 accumulation of the corresponding murine subset of monocytes associated with reduced  
433 steatohepatitis and improved metabolic parameters. Several studies have reported on the  
434 use of a variety of pharmaceutical inhibitors of CCR2 in murine fatty liver disease,  
435 administered in a variety of routes and in a variety of disease models (21, 27, 33). The  
436 human data presented here confirm that CCR2 antagonism may be of benefit in

437 NAFLD and indeed a phase II trial of a joint CCR2/CCR5 inhibitor, cencriviroc,  
438 reported in 2016 showing benefit on hepatic fibrosis (10). The recently published results of  
439 the dual CCR2/CCR5 inhibitor, cencriviroc, in clinical NAFLD show some changes in  
440 inflammatory activity and encouraging improvements in fibrosis compared to placebo treatment.  
441 The most obvious difference between CCX872 and cencriviroc is the additional effect on CCR5  
442 which may bring additional benefits in the setting of liver disease. Interestingly when cencriviroc  
443 was compared to CCX872 in the methionine-choline deficient diet model of steatohepatitis,  
444 greater improvement in ALT and fibrosis was observed with CCX872 (20), although the MCD is  
445 not noted for causing a great deal of fibrosis and also lacks relevance to human NAFLD. CCR2  
446 antagonists have been used in clinical trials in a variety of diseases where their use seems  
447 safe. Treatment of NAFLD would likely require administration over at least months and  
448 possibly years, and as such long-term safety is important. One important aspect of long-term  
449 use is the impact of CCR2 inhibition on carcinogenesis. Any effects are difficult to predict at  
450 present as animal models yield conflicting data (18), and CCR2 inhibition is being trialled for  
451 use in for example pancreatic cancer.

452

453 In conclusion, we suggest that a particular subset of monocytes is associated with  
454 progressive disease non-alcoholic fatty liver disease and that infiltration of liver by this subset  
455 is driven at least in part by CCL2/CCR2 signalling. Inhibition of this axis in NAFLD may be a  
456 rational means of improving hepatic and adipose tissue inflammation to prevent progressive  
457 liver disease.

## 458 **References**

- 459 1. Angulo, P. et al. Liver Fibrosis, but no Other Histologic Features, Associates  
460 with Long-term Outcomes of Patients With Nonalcoholic Fatty Liver Disease.  
461 *Gastroenterology* 2015
- 462 2. Armstrong, M. J. et al. Liraglutide efficacy and action in non-alcoholic  
463 steatohepatitis (LEAN): study protocol for a phase II multicentre, double-blinded,  
464 randomised, controlled trial. *BMJ open* 2013;3(11):e003995.

- 465 3. Armstrong, M. J. et al. Abdominal subcutaneous adipose tissue insulin  
466 resistance and lipolysis in patients with non-alcoholic steatohepatitis. *Diabetes Obes*  
467 *Metab* 2014;16(7):651-660.
- 468 4. Baeck, C. et al. Pharmacological inhibition of the chemokine CCL2 (MCP-1)  
469 diminishes liver macrophage infiltration and steatohepatitis in chronic hepatic injury.  
470 *Gut* 2012;61(3):416-426.
- 471 5. Boujedidi, H. et al. Housekeeping gene variability in the liver of alcoholic  
472 patients. *Alcoholism: Clinical and Experimental Research* 2012;36(2):258-266.
- 473 6. Browning, J. D. et al. Prevalence of hepatic steatosis in an urban population in  
474 the United States: impact of ethnicity. *Hepatology* 2004;40(6):1387-1395.
- 475 7. Charlton, M. et al. Fast food diet mouse: novel small animal model of NASH  
476 with ballooning, progressive fibrosis, and high physiological fidelity to the human  
477 condition. *American Journal of Physiology-Gastrointestinal and Liver Physiology*  
478 2011;301(5):G825-G834.
- 479 8. Cynis, H. et al. Inhibition of Glutamyl Cyclases alleviates CCL2-mediated  
480 inflammation of non-alcoholic fatty liver disease in mice. *Int J Exp Pathol*  
481 2013;94(3):217-225.
- 482 9. Ekstedt, M. et al. Fibrosis stage is the strongest predictor for disease-specific  
483 mortality in NAFLD after up to 33 years of follow-up. *Hepatology* 2014
- 484 10. Friedman, S. L. et al. Antifibrotic effects of the dual CCR2/CCR5 antagonist  
485 cenicriviroc in animal models of liver and kidney fibrosis. *HEpatology* 2017e0158156.
- 486 11. Gadd, V. L. et al. The portal inflammatory infiltrate and ductular reaction in  
487 human nonalcoholic fatty liver disease. *Hepatology* 2014;59(4):1393-1405.
- 488 12. Haukeland, J. W. et al. Systemic inflammation in nonalcoholic fatty liver  
489 disease is characterized by elevated levels of CCL2. *Journal of hepatology*  
490 2006;44(6):1167-1174.
- 491 13. Kanda, H. et al. MCP-1 contributes to macrophage infiltration into adipose  
492 tissue, insulin resistance, and hepatic steatosis in obesity. *Journal of Clinical*  
493 *Investigation* 2006;116(6):1494-1505.
- 494 14. Kirovski, G. et al. Elevated systemic monocyte chemoattractant protein-1 in  
495 hepatic steatosis without significant hepatic inflammation. *Exp Mol Pathol*  
496 2011;91(3):780-783.
- 497 15. Kleiner, D. E. et al. Design and validation of a histological scoring system for  
498 nonalcoholic fatty liver disease. *Hepatology* 2005;41(6):1313-1321.
- 499 16. Kohli, R. et al. High-fructose, medium chain trans fat diet induces liver  
500 fibrosis and elevates plasma coenzyme Q9 in a novel murine model of obesity and  
501 nonalcoholic steatohepatitis. *Hepatology* 2010;52(3):934-944.
- 502 17. Lefebvre, E. et al. Antifibrotic Effects of the Dual CCR2/CCR5 Antagonist  
503 Cenicriviroc in Animal Models of Liver and Kidney Fibrosis. *PLoS One* 2016;27 (11)
- 504 18. Li, M. et al. A role for CCL2 in both tumor progression and  
505 immunosurveillance. *Oncoimmunology* 2013

- 506 19. Lumeng, C. N., Bodzin, J. L., and Saltiel, A. R. Obesity induces a phenotypic  
507 switch in adipose tissue macrophage polarization. *Journal of Clinical Investigation*  
508 2007;117(1):175-184.
- 509 20. Miao, Z. et al. Reduction of Liver Fibrosis by CCR2 antagonist CCX872 in  
510 Murine Models of NASH. *Hepatology* 2016;SI
- 511 21. Miura, K. et al. Hepatic recruitment of macrophages promotes nonalcoholic  
512 steatohepatitis through CCR2. *Am J Physiol Gastrointest Liver Physiol*  
513 2012;302(11):G1310-21.
- 514 22. Nguyen, M. T. A., Favelyukis, S., and Nguyen..., A. K. A subpopulation of  
515 macrophages infiltrates hypertrophic adipose tissue and is activated by free fatty  
516 acids via Toll-like receptors 2 and 4 and JNK-dependent .... *Journal of Biological ...*  
517 2007
- 518 23. Obstfeld, A. E. et al. CC chemokine receptor 2 (CCR2) regulates the hepatic  
519 recruitment of myeloid cells that promote obesity-induced hepatic steatosis.  
520 *Diabetes* 2010;59(4):916-925.
- 521 24. Ouyang, X. et al. Fructose consumption as a risk factor for non-alcoholic fatty  
522 liver disease. *Journal of hepatology* 2008;48(6):993-999.
- 523 25. Parker, R., Hodson, J., and Rowe, I. A. C. Systematic Review: Current  
524 Evidence in Non-Alcoholic Fatty Liver Disease Lacks Relevance to Patients with  
525 Advanced Fibrosis. *Journal of Gastroenterology and hepatology* 2016
- 526 26. Patsouris, D. et al. Ablation of CD11c-positive cells normalizes insulin  
527 sensitivity in obese insulin resistant animals. *Cell metabolism* 2008;8(4):301-309.
- 528 27. Tamura, Y. et al. CC chemokine receptor 2 inhibitor improves diet-induced  
529 development of insulin resistance and hepatic steatosis in mice. *Journal of*  
530 *atherosclerosis and thrombosis* 2010;17(3):219-228.
- 531 28. Tamura, Y. et al. Inhibition of CCR2 ameliorates insulin resistance and  
532 hepatic steatosis in db/db mice. *Arteriosclerosis, thrombosis, and vascular biology*  
533 2008;28(12):2195-2201.
- 534 29. Weisberg, S. P. et al. CCR2 modulates inflammatory and metabolic effects of  
535 high-fat feeding. *Journal of Clinical Investigation* 2006;116(1):115-124.
- 536 30. Wentworth, J. M. et al. Pro-inflammatory CD11c+ CD206+ adipose tissue  
537 macrophages are associated with insulin resistance in human obesity. *Diabetes*  
538 2010;59(7):1648-1656.
- 539 31. Williams, C. D. et al. Prevalence of nonalcoholic fatty liver disease and  
540 nonalcoholic steatohepatitis among a largely middle-aged population utilizing  
541 ultrasound and liver biopsy: a prospective study. *Gastroenterology* 2011;140(1):124-  
542 131.
- 543 32. Wong, R. J., Cheung, R., and Ahmed, A. Nonalcoholic steatohepatitis is the  
544 most rapidly growing indication for liver transplantation in patients with  
545 hepatocellular carcinoma in the US. *Hepatology* 2014;59(6):2188-2195.
- 546 33. Yang, S. J. et al. Inhibition of the chemokine (C-C motif) ligand 2/chemokine  
547 (C-C motif) receptor 2 pathway attenuates hyperglycaemia and inflammation in a  
548 mouse model of hepatic steatosis and lipoatrophy. *Diabetologia* 2009;52(5):972-981.



550 **Table 1:** characteristics of cohorts used for human studies

	<b>Age</b> Years	<b>BMI</b> Kg/m <sup>2</sup>	<b>ALT</b> IU/L	<b>Diabetes</b> prevalence
Serum				
NOBLES	55.1	33.9	56.1	58%
LEAN	51.0	36.0	71.5	33%
Liver tissue				
NASH cirrhosis	56.9	32.7	37.5	88%
non-NASH cirrhosis	55.3	29.3	34.1	14%
Normal	57.5	27.3	20.0	0%

551

552 **Table 2:** correlation of frequency of intrahepatic CD11c<sup>+</sup>CD206<sup>+</sup> monocytes with clinical

553 parameters

	Correlation with intrahepatic CD11c <sup>+</sup> CD206 <sup>+</sup> monocytes (as % of CD14 <sup>+</sup> ) (r <sup>2</sup> )	p value
HbA1c	0.50	<0.001
ALT	0.02	0.551
BMI	0.04	0.388
Age	0.16	0.084

554

555



556 **Figure legends**

557

558 **Figure 1:** CD11c<sup>+</sup>CD206<sup>+</sup> monocytes are enriched in liver tissue. **A, B** gating strategy to  
559 identify CD45<sup>+</sup>CD14<sup>+</sup> monocytes. Representative samples of **(C)** peripheral blood and **(D)**  
560 liver infiltrating monocytes from the same individual **(E)**. Liver tissue from patients with  
561 NAFLD (n=8) showed a greater proportion of CD11c<sup>+</sup>CD206<sup>+</sup> monocytes as a proportion  
562 of CD45<sup>+</sup>CD14<sup>+</sup> monocytes, compared to other chronic liver disease (ALD n=4, PSC =3,  
563 PBC n=2, haemochromotosis n=1, cryptogenic cirrhosis n=1) or normal liver (n=5) (\*p<0.05  
564 by Kruskal-Wallis). **(F)** Mean fluorescence intensity of CD11c<sup>+</sup>CD206<sup>+</sup> cells by liver disease  
565 (Kruskal-Wallis p=0.056).

566

567 **Figure 2:** Monocytes were isolated from liver tissue from patients with or without NAFLD  
568 and analysed by flow cytometry. **A** The frequency of CD11c<sup>+</sup>CD206<sup>+</sup> monocytes in liver  
569 tissue correlated with insulin resistance, measured by HbA1c. n=24, r<sup>2</sup> = 0.499. **B** CCR2  
570 percentage expression was greater on CD14<sup>++</sup>CD16<sup>-</sup> monocytes with a non-significant  
571 reduction of CCR2 expression on all intra-hepatic monocytes.

572

573 **Figure 3:** Monocytes were isolated from liver tissue and analysed by flow cytometry. CCR2  
574 expression was higher on CD11c<sup>+</sup>CD206<sup>+</sup> monocytes isolated from NAFLD liver tissue  
575 (n=8) compared to non-NAFLD cirrhosis (n=11) or normal liver tissue (n=5) with regard to  
576 **A** percentage of CCR2<sup>+</sup> cells (normal, median 39.4% IQR 40.1, non-NAFLD cirrhosis 59.7%  
577 IQR 24.9, NAFLD 80.1% IQR 24.7) **and** mean fluorescent intensity (normal 171 IQR 163.7,  
578 non-NAFLD cirrhosis 200.6 IQR 80.1, NAFLD 3299 IQR 144.4). Data shown as median and  
579 IQR, n=23 in each case. \*p<0.05 by Mann-Whitney test

580

581

582 **Figure 4:** **A** RNA was isolated from liver tissue and CCL2 gene expression analysed by  
583 semi-quantitative PCR. CCL2 gene expression was significantly increased in liver tissue from  
584 patients with NASH (n=6) compared to normal liver tissue (n=6) (Mann Whitney test  
585  $p<0.01$ ). **B** Serum concentration of CCL2 measured by ELISA was higher in NAFLD (n=20)  
586 compared to healthy volunteers (n=10) (Mann Whitney test  $p<0.05$ ) **C** serum concentration  
587 of CCL2 increased with increasing disease activity as measured by the NAS score (one way  
588 ANOVA  $p<0.05$ ) **D** no relation was seen with fibrosis stage (one way ANOVA  $p>0.05$ )

589

590 **Figure 5:** Improvements in steatohepatitis with inhibition of CCR2. Thirteen animals in each  
591 group were given HFD with daily administration of vehicle or CCX872, and a further 8  
592 animals were given a control diet for 16 weeks. Triglyceride content was measured with a  
593 colorimetric assay. CCR2 inhibition reduced triglyceride accumulation ( $*p<0.05$ ,  $**p<0.01$  by  
594 students t-test). **B** CCR2 inhibition reduced serum ALT ( $*p<0.05$  by student's t-test).  
595 Histological assessment of liver disease confirmed reduced steatosis, as assessed by area of  
596 staining, panel C, but no differences in **D** histological inflammation or **E** histological fibrosis

597

598 **Figure 6:** Myeloid cells from liver and adipose tissue from mice given a high fat diet were  
599 analysed by flow cytometry. Treatment with a small molecule inhibitor of CCR2 did not  
600 affect proportions of **A** intrahepatic CD11b+F4/80hi Kupffer cells or **B** overall infiltrating  
601 CD11b+F4/80low monocytes (Mann-Whitney test to compare vehicle and CCX872 groups,  
602  $*p>0.05$ ). CCR2 antagonism reduced infiltration of CD11c+F4/80+ cells into **C** liver tissue  
603 (Mann-Whitney test to compare vehicle and CCX872 groups,  $*p<0.05$ ) and **D** adipose  
604 tissue (Mann-Whitney test to compare vehicle and CCX872 groups, t-test  $p<0.05$ ). Data are  
605 shown as boxes to denote IQR with line at median and whiskers showing maximum and  
606 minimum values.

607

608 **Figure 7:** Myeloid cells from liver and adipose tissue from mice given a high fat diet  
609 were analysed by flow cytometry. Treatment with a small molecule inhibitor of CCR2  
610 reduced hepatic infiltration with CCR2<sup>+</sup> CD11b<sup>+</sup>F4/80<sup>lo</sup> monocytes (student's t-test  
611 p<0.05) and **B** infiltration of liver tissue by pro-inflammatory Ly6c<sup>hi</sup> cells (\*\*p<0.05 by  
612 student's t-test)

613

614 **Figure 8:** 22 C57/Bl6 mice were fed HFD with 30% fructose in drinking water, or control  
615 diet without fructose, for 32 weeks. CCR2 antagonism with a small molecule inhibitor,  
616 CCX872, reduced fibrosis compared to vehicle control. Representative pictures of liver  
617 sections from **A** control and **B** CCX872-treated animals. **C** Fibrosis as assessed by  
618 percentage collagen area by Sirius red staining of liver sections. Data are shown as mean and  
619 SEM \*\*p<0.05 by student's t-test

620

621 **Figure 9:** CCR2 antagonism improved glycaemic control in mice on a HFD with CCR2.  
622 Glycaemic control was assessed at the beginning and end of the treatment period  
623 with glucose tolerance tests and insulin challenges. Mice in each group were showed  
624 similar responses at the start of the treatment period (A, D). At the time of sacrifice  
625 mice treated with CCX872 showed significantly improved response to glucose and  
626 insulin (B, E). When assessed by measuring area under the curve statistically  
627 significant changes were seen (C, F). \*\*\*p<0.001 by student's t-test.

628

629

630

631

632

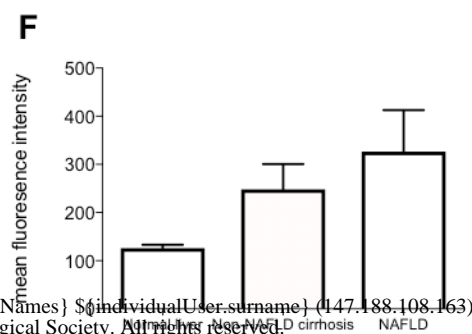
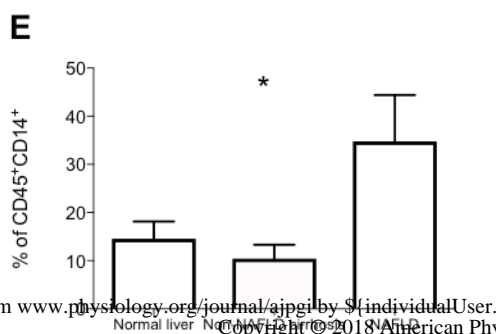
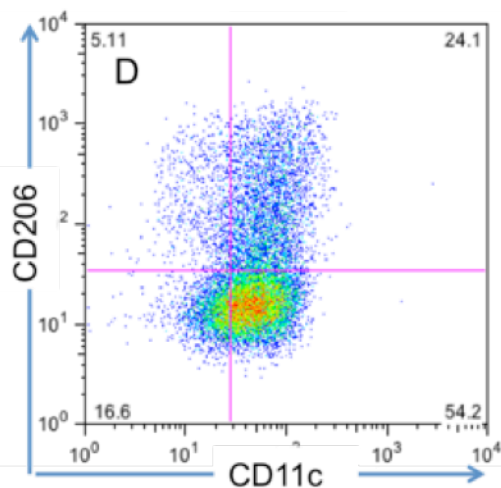
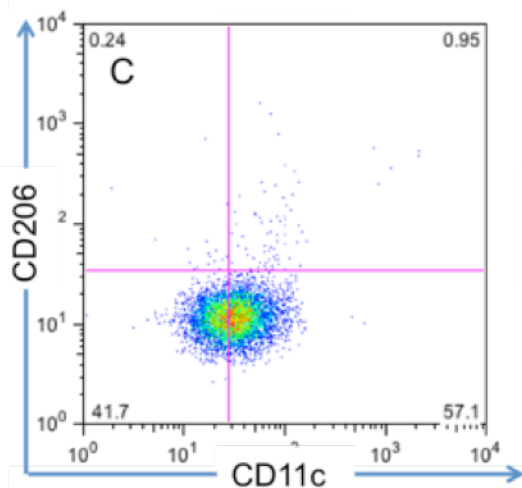
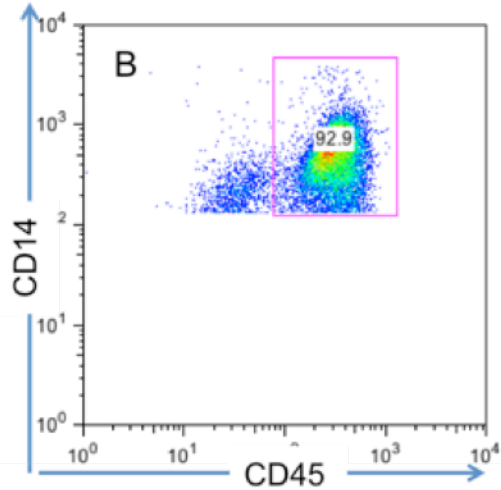
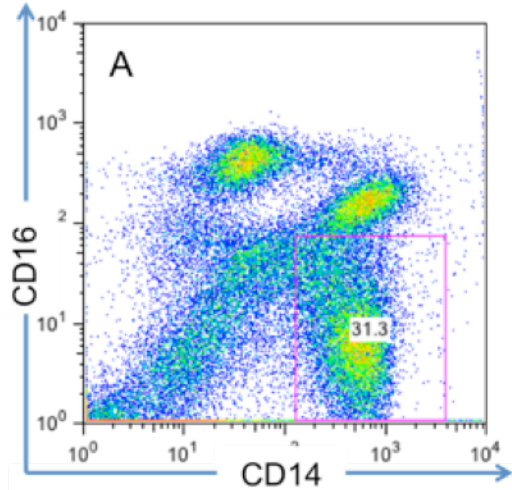
633

634

635

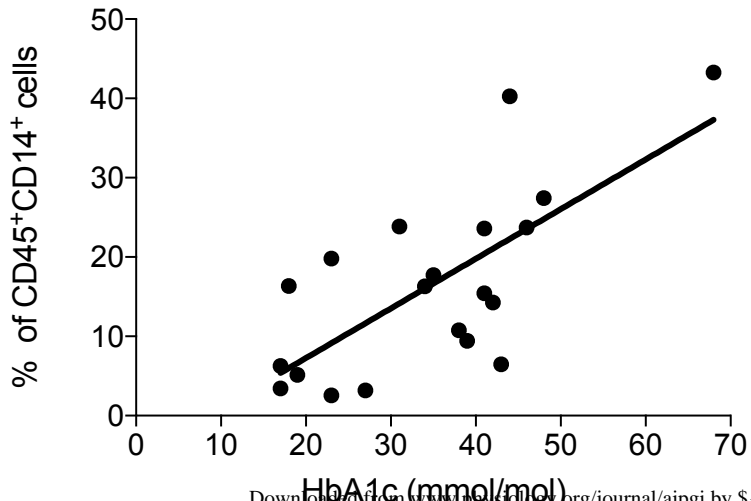
636

637



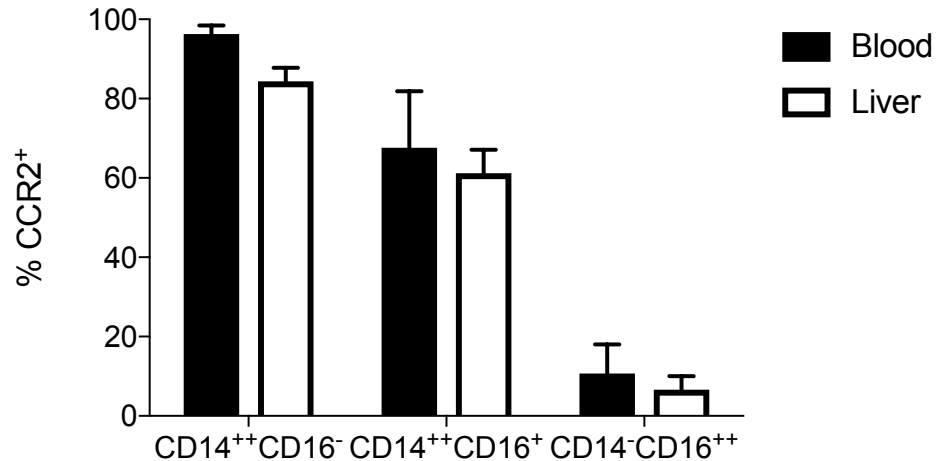
# A

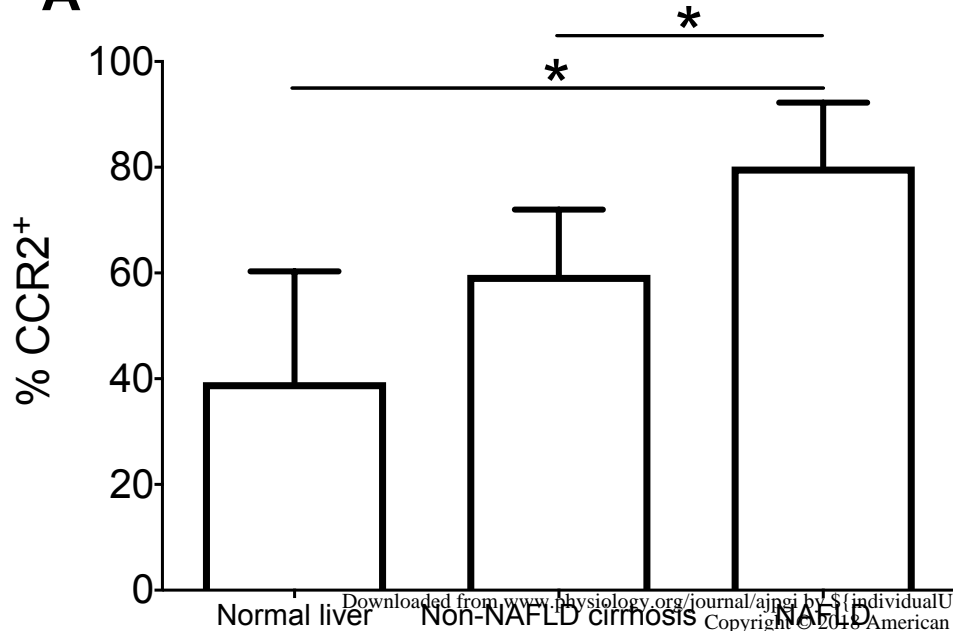
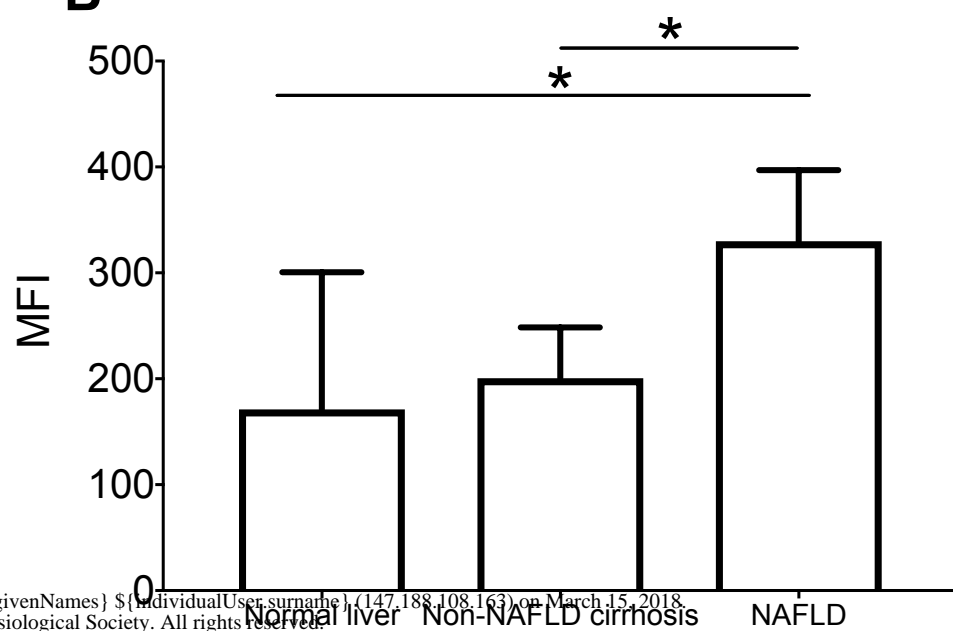
## Frequency of CD11c<sup>+</sup>CD206<sup>+</sup> by HbA1c

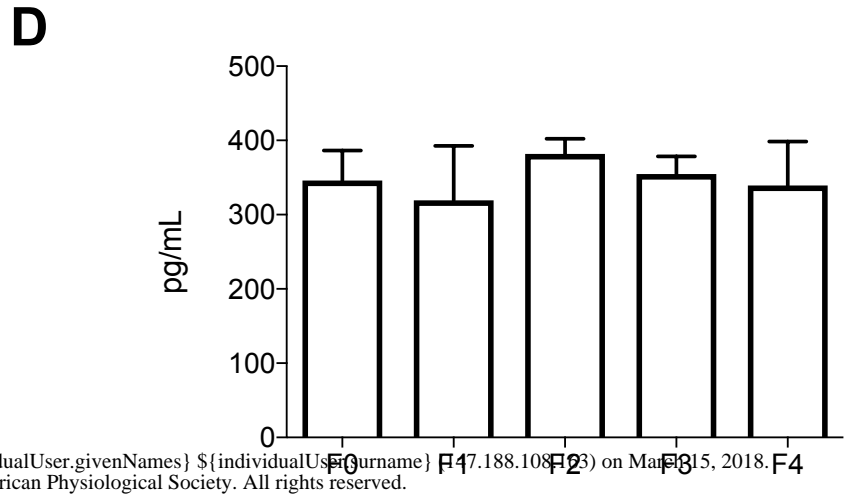
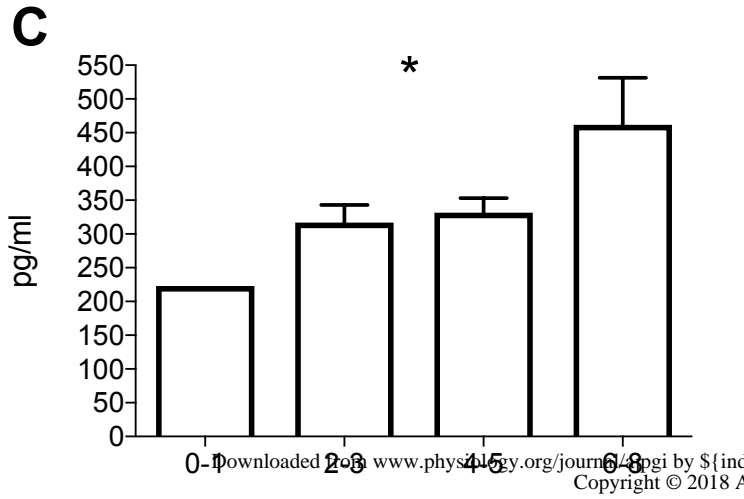
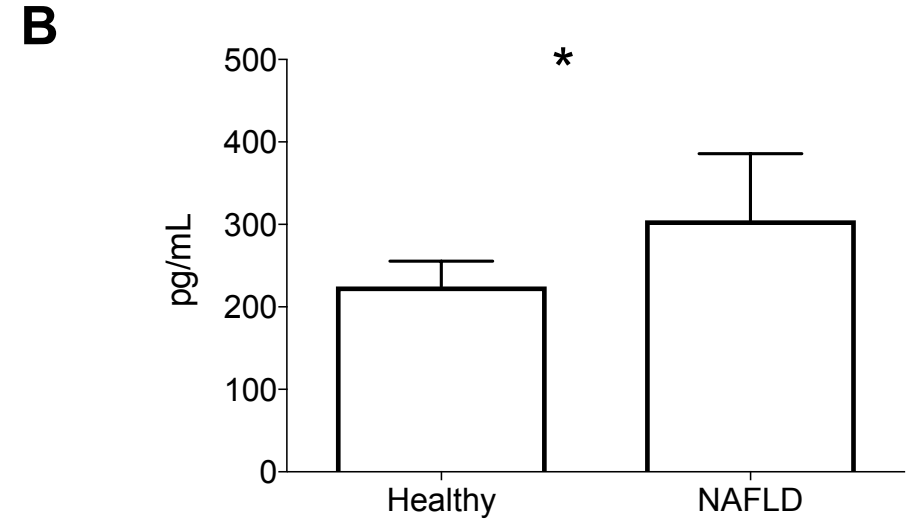
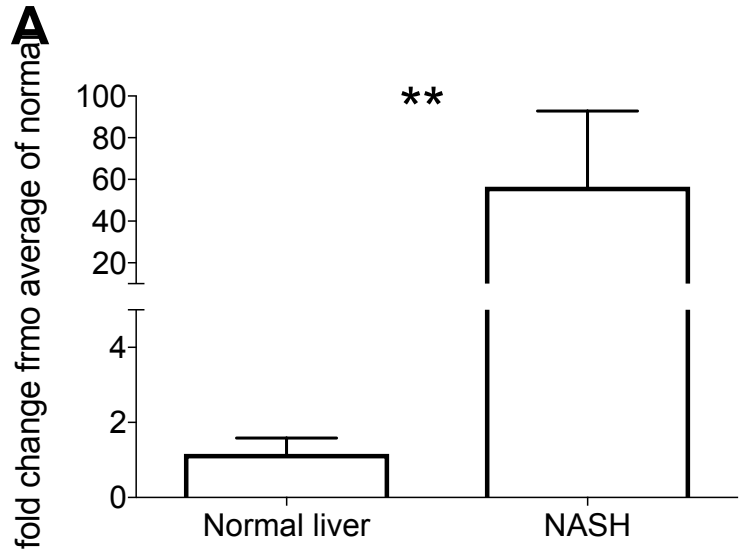


# B

## CCR2 expression - %



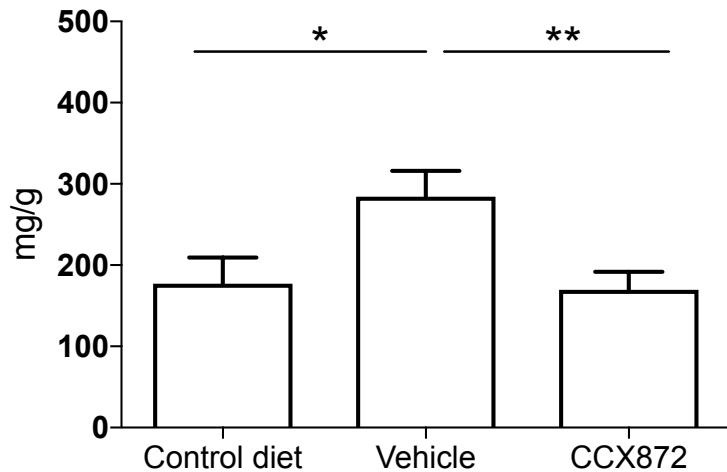
**A****B**



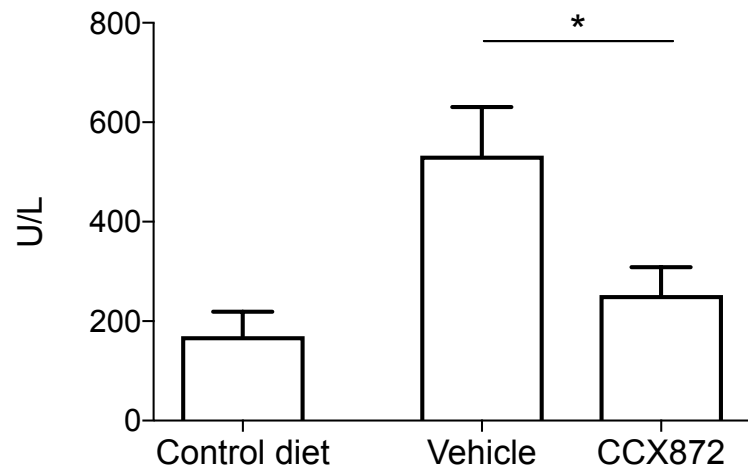


**A**

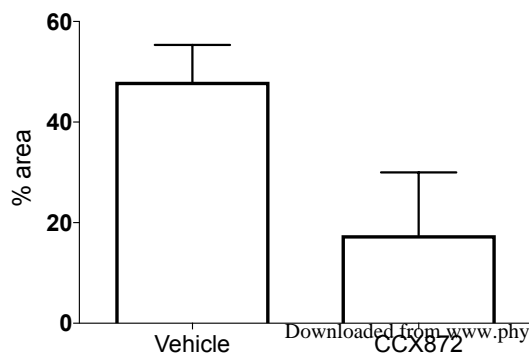
## HFD: Liver triglyceride content

**B**

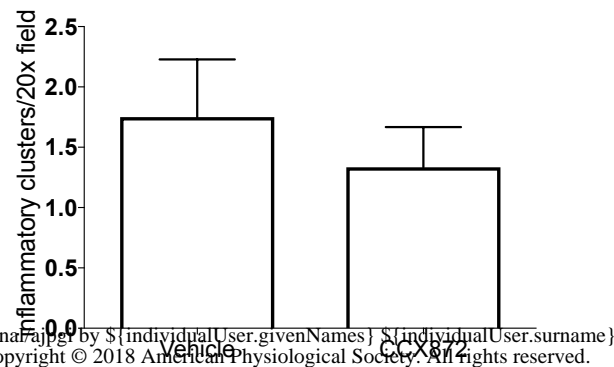
## Alanine aminotransferase

**C**

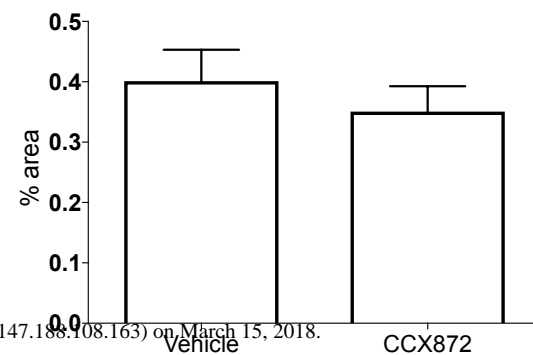
## Histology: steatosis by area

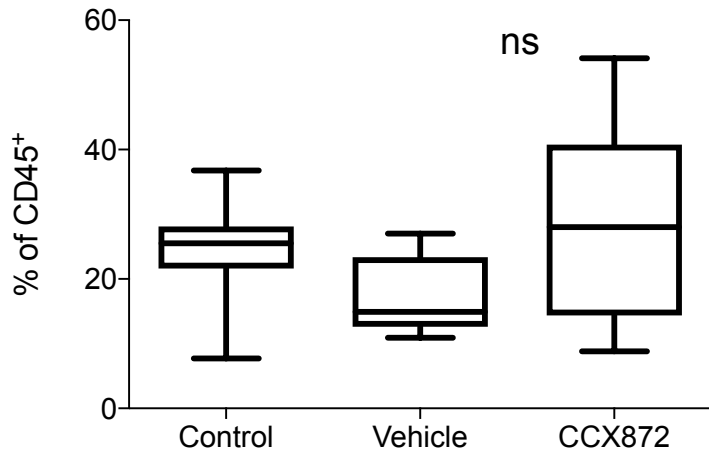
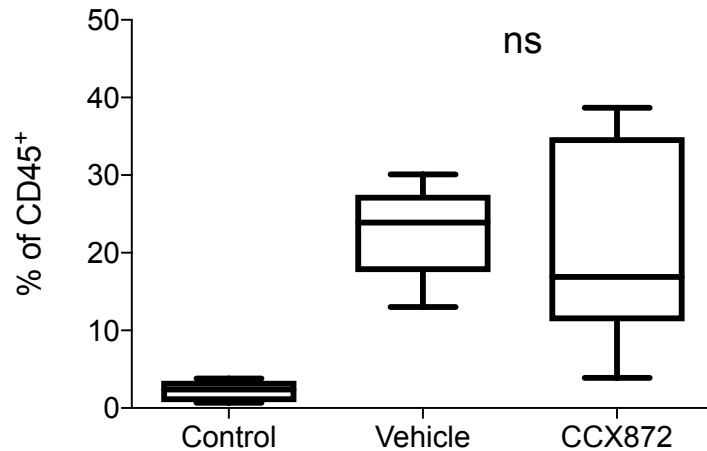
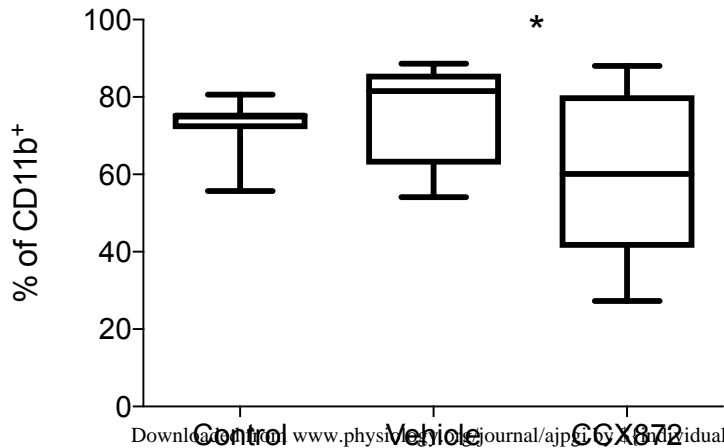
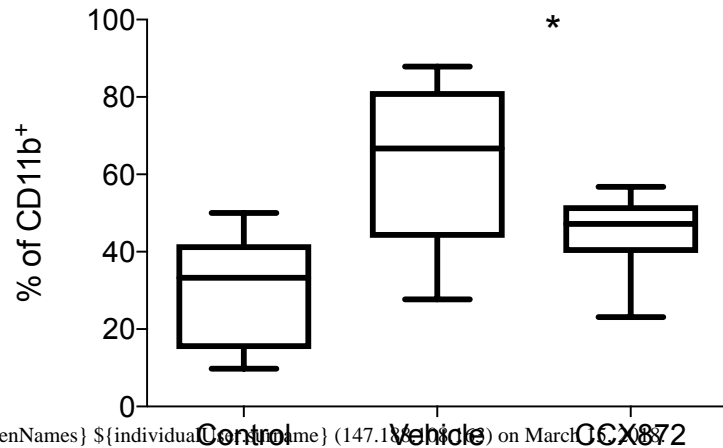
**D**

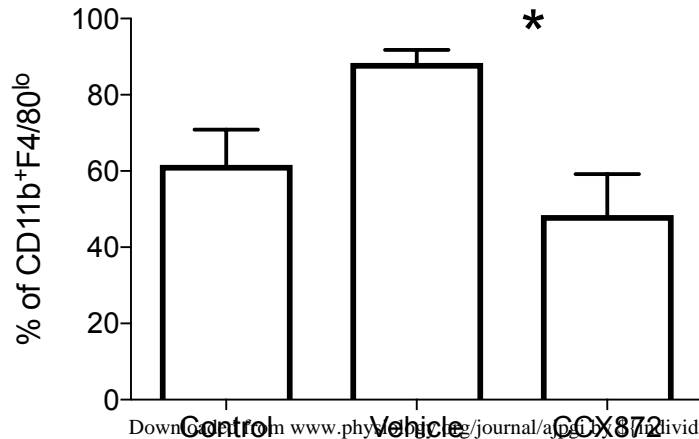
## Lobular inflammation

**E**

## Fibrosis by area



**A** Intrahepatic resident Kupffer Cells**B** Intrahepatic infiltrating monocytes**C** Intrahepatic CD11c<sup>+</sup>F4/80<sup>+</sup>**D** Adipose tissue CD11c<sup>+</sup>F4/80<sup>+</sup>

**A**CCR2<sup>+</sup> infiltrating CD11b<sup>+</sup>F4/80<sup>lo</sup> monocytes**B**Intrahepatic Ly6c<sup>hi</sup> monocytes